

pubs.acs.org/JPCB Article

Structure Relaxation Approximation (SRA) for Elucidation of Protein Structures from Ion Mobility Measurements (II). Protein Complexes

Published as part of The Journal of Physical Chemistry virtual special issue "Early-Career and Emerging Researchers in Physical Chemistry Volume 2".

Tyler C. Cropley, Fanny C. Liu, Thais Pedrete, Md Amin Hossain, Jeffrey N. Agar, and Christian Bleiholder*



Cite This: J. Phys. Chem. B 2023, 127, 5553-5565



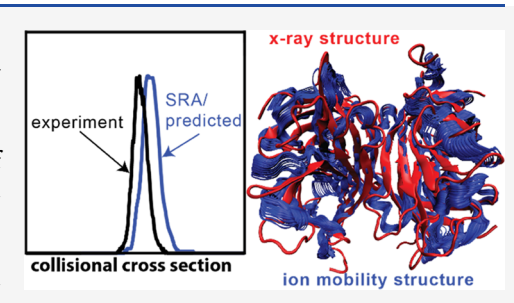
ACCESS

III Metrics & More

Article Recommendations

3 Supporting Information

ABSTRACT: Characterizing structures of protein complexes and their disease-related aberrations is essential to understanding molecular mechanisms of many biological processes. Electrospray ionization coupled with hybrid ion mobility/ mass spectrometry (ESI-IM/MS) methods offer sufficient sensitivity, sample throughput, and dynamic range to enable systematic structural characterization of proteomes. However, because ESI-IM/MS characterizes ionized protein systems in the gas phase, it generally remains unclear to what extent the protein ions characterized by IM/MS have retained their solution structures. Here, we discuss the first application of our computational structure relaxation approximation [Bleiholder, C.; et al. J. Phys. Chem. B 2019, 123 (13), 2756–2769] to assign



structures of protein complexes in the range from ~ 16 to ~ 60 kDa from their "native" IM/MS spectra. Our analysis shows that the computed IM/MS spectra agree with the experimental spectra within the errors of the methods. The structure relaxation approximation (SRA) indicates that native backbone contacts appear largely retained in the absence of solvent for the investigated protein complexes and charge states. Native contacts between polypeptide chains of the protein complex appear to be retained to a comparable extent as contacts within a folded polypeptide chain. Our computations also indicate that the hallmark "compaction" often observed for protein systems in native IM/MS measurements appears to be a poor indicator of the extent to which native residue—residue interactions are lost in the absence of solvent. Further, the SRA indicates that structural reorganization of the protein systems in IM/MS measurements appears driven largely by remodeling of the protein surface that increases its hydrophobic content by approximately 10%. For the systems studied here, this remodeling of the protein surface appears to occur mainly by structural reorganization of surface-associated hydrophilic amino acid residues not associated with β -strand secondary structure elements. Properties related to the internal protein structure, as assessed by void volume or packing density, appear unaffected by remodeling of the surface. Taken together, the structural reorganization of the protein surface appears to be generic in nature and to sufficiently stabilize protein structures to render them metastable on the time scale of IM/MS measurements.

■ INTRODUCTION

Protein complexes carry out most cellular functions, ^{1,2} from cellular signaling mediated by transient protein complexes³ to the production of proteins by the ribosomal protein machinery. ⁴ Structural perturbations of protein complexes often alter their ability to carry out their designated functions and may lead to disease phenotypes. ^{5,6} For example, mutations of transthyretin may promote non-native assembly states and the drug tafamidis acts to prevent formation of such misfolded states by stabilizing transthyretin tetramers. ⁷ Thus, characterizing structures of protein complexes and their disease-related aberrations is essential to understanding the molecular mechanisms of many disease-related biological processes.

Nevertheless, our understanding of how structural changes of protein complexes affect their function and dysfunction in biological systems remains limited. In part, this gap in our understanding arises from traditional biophysical approaches being most effective when investigating isolated, purified protein systems without intrinsic disorder. For example, X-ray and NMR spectroscopy have been applied with great success to characterize protein conformational states. 8–12 However, X-ray spectroscopy requires conditions under which the protein crystallizes and NMR works best at sample concentrations that can be significantly higher than physiological concentrations. As a result, assemblies may be formed

Received: February 14, 2023 Revised: May 20, 2023 Published: June 13, 2023





that may not be biologically relevant. For example, the toxicity of ALS-associated variants of Cu/Zn superoxide dismutase (SOD1) requires dissociation of the SOD1 dimer. This reaction has a dissociation constant K_D in the low micromolar range, which is accessible to MS but not to most NMR experiments. 13 Traditional methods are also limited in their abilities to characterize structurally heterogeneous systems where transiently populated species interconvert. By contrast, many biological phenomena, from glycosylated proteins 14,15 to protein assemblies implicated in cellular signaling 16,17 or neurodegenerative diseases, 14,18-21 involve steady states of transiently populated species that often are structurally heterogeneous and flexible. Further challenges to traditional biophysical methods arise when protein function in the context of biological cells, where processes are carried out collectively by all proteins present in a cell ("proteome") and are best described by protein-protein interaction networks ("interactome").22-

Hybrid ion mobility/mass spectrometry (IM/MS) methods exhibit sufficient sensitivity, sample throughput, and dynamic range to enable large-scale systematic measurements of proteomes.²⁹⁻³⁴ However, these methods suffer from two major shortcomings when attempting to characterize the solution-phase structural heterogeneity of protein systems. First, because IM/MS characterizes ionized protein systems in the gas phase, it generally remains unclear to what extent the protein ions characterized by IM/MS have retained their solution structures. 35,36 While it is becoming apparent that IM/MS measurements are nonergodic³⁷ and protein solution structures are metastable in the absence of solvent, 37-45 it remains unclear which structural aspects are retained and which are not. There is further ample evidence that protein complexes generally retain aspects of their native structure, 2,46-53 but it remains underexplored to what extent interfaces between the distinct polypeptide chains, ligandbinding sites, or allosteric sites remain preserved in the IM/MS measurement. The major challenge here is to elucidate structural details from IM/MS data that characterize protein conformations by their orientationally averaged mean "effective area" termed "collision cross section". 54-5

To enable reliable structural interpretation of IM/MS spectra for protein systems, we developed the structure relaxation approximation (SRA) method.³⁷ The SRA was developed to predict how an ensemble of protein solution structures would adopt to the gas-phase environment of an IM/MS experiment such that structural changes caused by the charge state and absence of solvent are not underestimated nor overestimated. Originally formulated for monomeric proteins, 37,39 the SRA is a large-scale computational method that reliably assigns protein structures to IM/MS spectra. The central idea of the SRA is that the more charge states and experimental conditions are probed by experiment and theory, the greater the confidence of the structural interpretation because chance agreement for all conditions and charge states becomes increasingly unlikely. The key aspects of the SRA method are (1) to probe structural relaxation caused by absence of solvent for an ensemble of protein solution structures, (2) to predict ion mobility spectra through accounting for the structural relaxation that protein systems undergo during the IM/MS measurement, (3) to predict ion mobility spectra for all charge states experimentally observed for the protein systems, and (4) to consider various protonation site isomers of all titratable amino acid residues based on solvent accessibility.

We successfully applied the SRA to characterize structures of small monomeric proteins detected by IM/MS, such as ubiquitin³⁷ and CCL5.³⁹ The main outcome of these studies was that monomeric, globular proteins retain a high degree of their native solution-phase backbone residue—residue contacts during an IM/MS measurement. Native salt bridges were found to largely remain intact and stabilize the protein structure in the gas-phase environment of the IM/MS instrument in accord with prior literature on this topic.^{57–61} However, the SRA also indicated that native contacts within structurally flexible regions, such as loops or terminal regions of polypeptide chains that are not tethered to other regions by intermolecular bonds, are largely lost during the IM/MS measurement.

Prior computational analysis of experimental IM/MS spectra indicated that native structures of protein complexes can largely be retained during IM/MS. 50,52 Furthermore, structural reorganization in the absence of solvent molecules was proposed to be largely restricted to the orientations of amino acid side chains to self-solvate charged and hydrophilic moieties, effectively resulting in a smoother protein surface. However, protein complexes contain structurally important grooves and cavities and it remains underexplored to what extent these regions would be retained in IM/MS. Hence, a clearer understanding of how these regions restructure in the absence of solvent appears crucial for efforts that seek to characterize protein complex structures using IM/MS as well as those that seek to employ MS-based techniques for preparative purposes. 62,63

Here, we describe the application of the SRA method to the structural interpretation of protein complexes from IM/MS data. We demonstrate that the SRA method is capable to predict charge-state-specific ion mobility spectra for protein dimers of the chemokine C-C motif ligand 5 (CCL5/ RANTES) and superoxide dismutase 1 (SOD1) and the neutravidin and streptavidin tetramers ranging from ~15 to ~60 kDa. We discuss which aspects of the solution-phase structure of these protein complexes are retained and discuss how changes to the protein backbone contribute to the compaction observed in IM/MS measurements. Our main conclusions are that structural reorganization of these protein systems is (1) driven by a modest 10% increase in hydrophobic content of their surface areas and (2) associated mainly by the reorientation of hydrophilic, solvent-exposed residues not part of β -strand secondary structure elements. This remodeling of the protein surfaces appears to sufficiently stabilize their structures to render them metastable on the time scale of IM/ MS experiments.

■ EXPERIMENTAL AND COMPUTATIONAL DETAILS

Sample Preparation. Human CCL5 was purchased from PeproTech (Cranbury, NJ). SOD1 from human erythrocytes was purchased from Sigma-Aldrich (St. Louis, MO). As purchased, SOD1 contains an artifactual polysulfane bridge between two Cys111 of the dimer. SOD1 is prepared for direct infusion electrospray ionization (ESI) as described previously. Briefly, sulfane sulfur is cleaved by dithiothreitol using conditions optimized not to cleave SOD1's intrasubunit disulfide, and then removed by ultrafiltration. The removal of sulfane sulfur and the integrity of the intrasubunit disulfide are confirmed by intact mass measurement on a 9.4 T Fourier

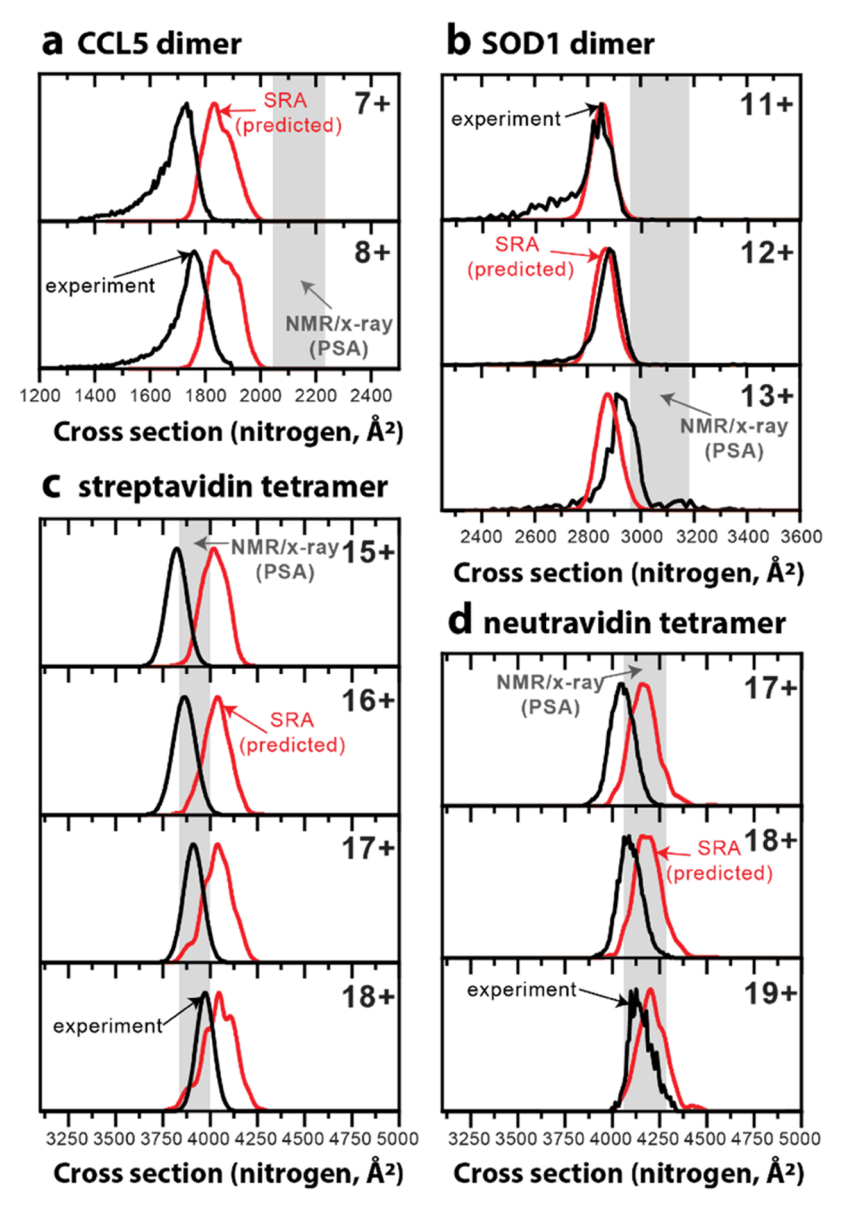


Figure 1. Comparison between experimental ion mobility spectra (black traces) and spectra predicted by the SRA (nitrogen buffer gas) for (a) CCL5 dimers, (b) SOD1 dimers, (c) streptavidin tetramers, and (d) neutravidin tetramers (red traces). Agreement between the experimental and predicted spectra are within the errors of theoretical methods (RMSD $\sim 3.5\%$). Cross sections expected for the X-ray/NMR structures (shaded) indicate a compaction for CCL5 and SOD1 with respect to their native structures. Calculated cross sections for the different X-ray/NMR structures can be found in the Supporting Information (Table S4), and the width of the shaded area reflects the range of the calculated cross sections.

transform ion cyclotron resonance MS (Bruker Daltonics). Ammonium acetate salt, acetic acid, and recombinant streptavidin and neutravidin from egg whites were purchased from Thermo Fisher Scientific (Waltham, MA). Water used in sample preparations was LC/MS grade quality and was purchased from Sigma-Aldrich (St. Louis, MO). CCL5 samples were diluted to achieve a concentration of 10 μM in LC/MS grade water with 10 v % acetic acid. SOD1 was diluted to 10 µM in 200 mM ammonium acetate. Neutravidin was desalted using a 3 kDa Amicon Ultra centrifugal filter (Millipore Sigma, Burlington, MA) and diluted to achieve a concentration of 60 µM in 10 mM ammonium acetate. Streptavidin was buffer exchanged from tris buffer to ammonium acetate using a Micro Bio-Spin 6 column (Bio-Rad, Hercules, CA). After buffer exchange samples were desalted using the same procedure as neutravidin. Streptavidin

samples were diluted to ${\sim}37~\mu\mathrm{M}$ in 10 mM ammonium acetate.

Tandem-TIMS/MS Measurements. A full description of the experimental details is given in the Supporting Information. Briefly, ion mobility measurements were performed on the recently developed coaxial tandem-TIMS-QTOF instrument (tTIMS/MS) shown in Figures S1 and S2 with nitrogen buffer gas described elsewhere. Samples were loaded into a gastight syringe (Hamilton, 250 μ L) and directly infused into the electrospray ionization source (positive mode) at a flow rate of 180 μ L/h. Ions produced from ESI are deflected into the first TIMS analyzer (TIMS-1) where they are mobility separated. Ions were transmitted through the interface region and TIMS-2 before mass analysis. Mobility selection and collision-induced unfolding (CIU) of mobility-selected species were performed between aperture-1 and aperture-2 and between aperture-2

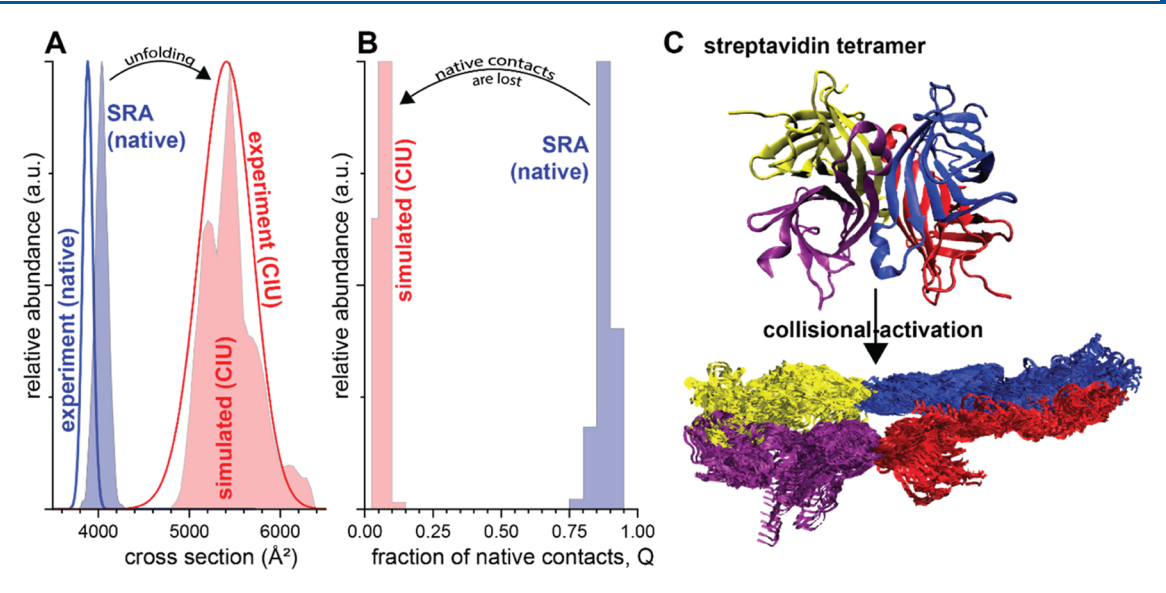


Figure 2. Collision-induced unfolding of streptavidin as a negative control. (a) Comparison of computed spectra for charge state 16+ of tetrameric streptavidin to experimental spectra from native and collisional-activated measurements. The comparison underlines that the simulated spectra reproduce the trends in the experiments due to collisional activation. (b) Fraction of native contacts for the simulated spectra under native (blue) and activated (red) conditions. The plot confirms that native contacts are not retained after CIU. (c) Cartoon highlighting the significant structural changes of the four streptavidin polypeptide chains (red, blue, yellow, purple) upon CIU.

deflector-2 (see Figure S2, Supporting Information), respectively, as described elsewhere. Cross sections were calibrated as described using perfluorinated phosphazenes contained in Agilent ESI tuning mix (m/z 922, 1522, 2122) with reported reduced ion mobilities (0.841, 0.642, 0.530 cm²/(Vs)).

Solution-Phase Molecular Dynamics (MD) Calculations. Initial structures were taken from the protein data bank (PDB; CCLS: PDB 1HRJ; SOD1: PDB 1PU0; streptavidin: PDB 1SWB; neutravidin: PDB 1AVD). Explicit-solvent molecular dynamics (MD) calculations were carried out for a total of 1.25 μ s with the GROMACS package in conjunction with the AMBER ff03 force field⁷¹ and the TIP3P⁷² solvent model under periodic boundary conditions as described elsewhere.³⁷ More details are found in section S2 of the Supporting Information.

Structure Relaxation Approximation (SRA) Calculations. Structure relaxation approximation (SRA) calculations were carried out as described.³⁷ Briefly, an ensemble of >1000 protein solution structures generated from explicit-solvent molecular dynamics simulations (see above) was (de)protonated to the experimentally observed charge states. Subsequently, short MD simulations were carried out to account for gas-phase relaxation of the ionized solution structures. The length and temperature of these short MD simulations were previously calibrated against a set of experimental IM/MS spectra.³⁷ Gas-phase MD simulations were carried out with GROMACS in conjunction with the OPLS/AA^{73,74} force field. The experimental charge states were attained by (de)protonating acidic and basic residues based on their solvent accessibility as described.³⁷ Details on the location of charged residues can be found in Figure S3 (Supporting Information). Collision-induced unfolding spectra were simulated by raising the temperature in steps of 50 K over time steps of 5 ns as described. 37,75 Solvent-accessible surface areas were calculated by the POPS algorithm.⁷⁶ The MOPAC⁷⁷ package was used for all electronic structure

calculations. The Protein Volume package was used to calculate molecular volumes. 78

Cross Section Calculations. Theoretical cross sections for protein model structures were computed by the projection superposition approximation (PSA) for nitrogen. S6,79–82 Approximately 15% of the 500 snapshots saved during the final simulation of the gas-phase relaxation simulations for each structure from the solution ensemble were used for cross section calculations as described. Overall, each SRA spectrum depicted in this work was constructed from approximately 112,500 individual cross section calculations.

RESULTS AND DISCUSSION

Native Residue-Residue Contacts of Protein Complexes Are Largely Preserved in the Absence of Solvent. In prior work, we successfully predicted chargestate-specific ion mobility spectra for two ~8 kDa monomeric proteins, ^{37,39} which indicated that their native salt bridges and hydrophobic cores as well as other native contacts are largely retained upon ESI-IM/MS. We observed substantial structural reorganization in the absence of solvent mainly for those regions of the polypeptide chain that were not tethered to other regions by intermolecular bonds. Our prior work also showed that reorganization of flexible regions of the CCL5 chain causes the measured CCL5 cross section to be significantly smaller than the cross section calculated for the NMR structure, i.e., the hallmark compaction 33,45,50,52,83 generally observed for protein systems in native IM/MS measurements. Considering prior work indicating marginal restructuring of the polypeptide backbone of protein complexes upon solvent removal in IM/MS, 50 it is unclear if these lessons gleaned from small monomeric proteins extrapolate to larger protein complexes nor is it obvious if the computational demand of the SRA lends itself to interpret structures of protein complexes from IM/MS spectra.

Figure 1 compares the experimentally measured native IM/MS spectra to the corresponding spectra predicted by the SRA method for the dimers of CCL5 (16 kDa) and SOD1 (32 kDa)

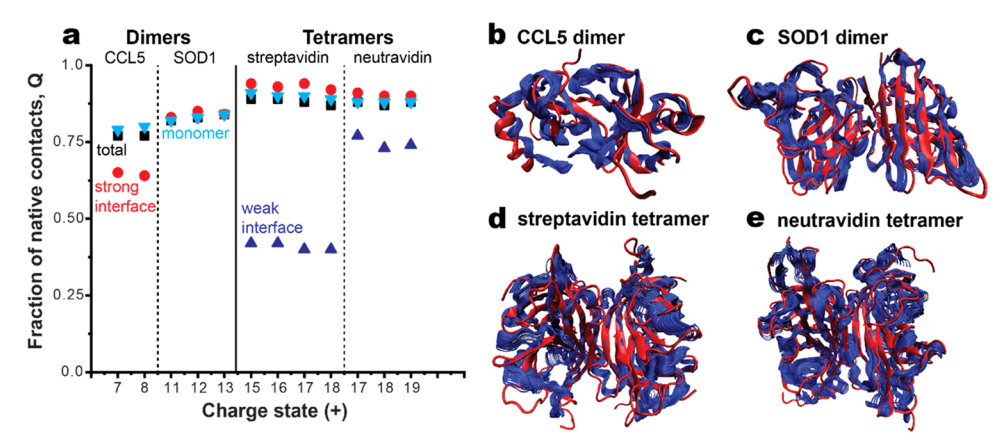


Figure 3. (a) Fraction of native contacts predicted by the SRA method for various charge states with respect to the total contacts (black square), contacts within monomer chains (light blue inverse triangles), contacts between strong interfaces (red circles), and contacts between weak subunit interfaces (dark blue triangles). Native contacts, except for the weakly bound subunit interface for streptavidin, appear largely retained in IM/MS measurements. (b)—(e) Ensemble of SRA-predicted structures (blue) superimposed onto the native structure obtained from NMR or X-ray (red) for the CCL5 dimer, SOD1 dimer, streptavidin tetramer, and neutravidin tetramer. The SRA indicates the overall native topologies are retained except for termini and regions containing loops.

as well as the tetramers of neutravidin (60 kDa) and streptavidin (53 kDa). The data reveal that the main features in the SRA-predicted spectra differ, on average, by approximately 3.5% from the main experimental feature (see Table S1 in the Supporting Information). The SRA-predicted spectra shown in Figure 1 do not randomly deviate from the experimental spectra. In line with our prior application of the SRA method to the monomeric protein ubiquitin,³⁷ the SRApredicted spectra tend to overestimate the experimental cross sections. As discussed, this systematic overestimation of cross sections most likely arises from (1) minor systematic errors of the PSA cross section calculation in nitrogen buffer gas and/or (2) minor overestimation of the structural relaxation process of the protein systems during the IM/MS measurement. The SOD1 spectra deviate from this general trend and appear much closer in agreement with the experimental data ($\sim 0-2\%$). While the reason for this better agreement is not currently known to us and warrants further investigations, we emphasize that the deviations are overall consistent with those we previously reported for monomeric proteins and compatible with the errors of the experimental and theoretical methods as discussed.37,39

As a negative control, we performed collision-induced unfolding (CIU) of charge state 16+ of the streptavidin tetramer and probed if our simulations reproduce the experimental trends (Figure 2). Experimentally, collisioninduced unfolding (CIU) of the tetramer was accomplished by placing 80 V between aperture-2 and deflector-2 (see Figure S2, Supporting Information) as described previously. 37,67 Figure 2a shows that the cross section of the streptavidin tetramer increases by roughly 30% from ~4000 to ~5500 Å². Computationally, the unfolding process was simulated as described previously^{37,52,75} by increasing the temperature of the MD simulations in steps of 50 K and 5 ns up to a final temperature of 850 K. Figure 2a underlines that the MD simulations reproduce the increase in cross section observed in the experimental CIU spectra, underlining the structural denaturation of the polypeptide chains and loss of native contacts due to collisional activation (Figure 2b,c).

Taken together, our analysis here indicates (1) that the SRA predicts charge-state-specific ion mobility spectra for protein

complexes within the errors of the computational and experimental methods and (2) that the structures of the protein complexes predicted by the SRA unlikely underestimate the structural reorganization the protein systems undergo in the IM/MS experiment. Hence, our analysis indicates that we can reliably use the SRA-predicted structures to assess the structural reorganization of the protein complexes during the IM/MS experiments. Further, our results suggest that the SRA method appears to be generally valid for prediction of charge-state-specific IM/MS spectra of protein systems for a range of masses and oligomeric states.

To assess the extent to which the protein complexes undergo restructuring of the backbone residue—residue interactions, we calculated the fraction of native backbone contacts, ⁸⁴ Q, for the structures of the protein complexes predicted by the SRA. We calculated Q with respect to the corresponding X-ray or NMR structures (PDB 1HRJ for CCLS dimers, PDB 1PU0 for SOD1 dimers, PDB 1SWB for streptavidin tetramers, and PDB 1AVD for neutravidin tetramers) and tabulated the results in Table S2 (Supporting Information).

Figure 3a shows the mean fraction of native contacts for the different charge states predicted by the SRA method for the CCL5 and SOD1 dimers and the neutravidin and streptavidin tetramers. The calculated fractions of native contacts (O \sim 0.75 to ~ 0.85) reveal that, overall, most of the native backbone residue-residue interactions are retained for all protein complexes studied here. The greatest loss of native backbone interactions is observed for the CCL5 dimer ($Q \sim 0.77$). However, this loss of native contacts is traced back to mainly arise from loss of native contacts related to the terminal amino acid residues because the fraction of native contacts is ~0.85 for the internal residues 10-60 (see Table S2, Supporting Information). These terminal regions, however, are flexible in solution and also poorly retained in monomeric CCL5.³⁹ The data further show that only minor changes of the fraction of native contacts are observed for increasing charge states of the same protein systems. This observation supports the notion that the charge state of the detected protein ions does not profoundly influence the retention of native interactions (in the absence of overt changes to the detected cross

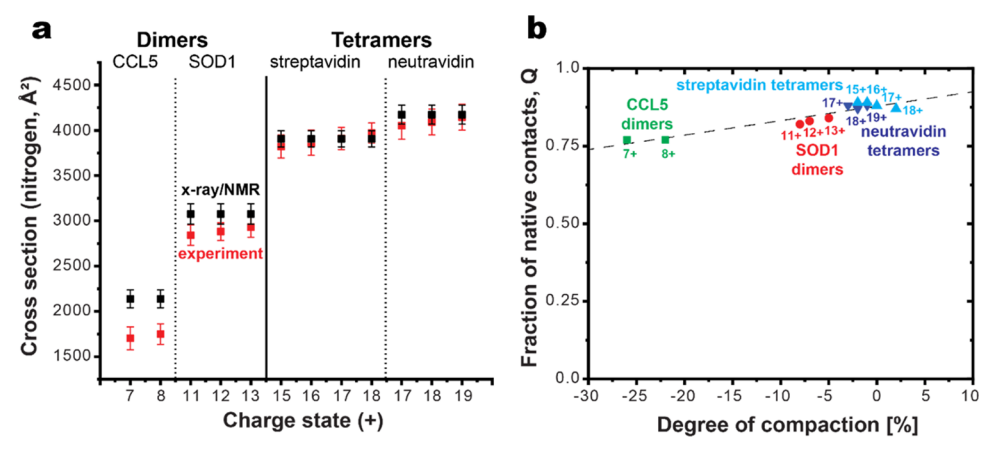


Figure 4. (a) Main features of the experimental (red square) cross section distribution and the average PSA cross section for a collection of X-ray/NMR structures (black square). Plotted are mean values and ranges represent full width at half maximum (FWHM) of experimental features (red error bars) and the standard deviation for the calculated PSA cross sections of available PDB entries (black error bars, see Supporting Information Table S4 for details). (b) Correlation between the fraction of native contacts and the compaction, i.e., the relative difference between experimental cross sections and those calculated for the X-ray/NMR structure for CCL5 dimers (green squares), SOD1 dimers (red circles), streptavidin tetramers (light blue triangles), and neutravidin tetramers (dark blue inverted triangles). Linear regression analysis (black dashed line) suggests compaction correlates weakly with loss of native contacts.

sections),^{46,50} which is expected until the point that the added protons are close enough to interact or disrupt salt bridges. Hence, overall, our observations support previous literature^{2,33,37,39,45–52} that proposes that significant structural reorganization of the native polypeptide chains of protein complexes is unlikely during native IM/MS measurements, except for flexible regions such as termini or loops.

An important but underexplored aspect is to what extent binding interfaces between distinct polypeptide chains undergo structural changes during IM/MS measurements. We expect that structural changes resulting from desolvation to affect binding interfaces less, to the extent that residues at a subunit interface are less hydrated than residues on a surface. To address this question, we calculated the fraction of native contacts for the residues composing the binding interfaces between the various protein chains with respect to their native X-ray and/or NMR structures (see Figure 3a and Table S2, Supporting Information, for details). The fractions of native contacts indicate that the binding interface between the two polypeptide chains of the CCL5 dimer retains ~65% of native contacts, whereas the SOD1 dimer retains more than 80%. We rationalize the comparatively poor retention of native interactions for the CCL5 dimer by the fact that the flexible N-terminal residues 1-10 dominate the interactions between the polypeptide chains of the CCL5 dimer. The neutravidin and streptavidin tetramers can be decomposed into a strongly and weakly bound dimer (an additional dimer can be extracted from the transverse protein chains, but these have little contact in the native structure and are thus disregarded for analysis here). The data plotted in Figure 3 indicate that native contacts are strongly retained for the strong binding interfaces within the neutravidin and streptavidin tetramers (Q > 0.90). By contrast, native contacts present in the weak interfaces are not retained as strongly, with streptavidin being generally more prone to structural changes than neutravidin ($Q \sim 0.4$ for weakly bound interface of streptavidin and $Q \sim 0.75$ for that of neutravidin).

Taken together, the fraction of native contacts calculated for the structures predicted by the SRA method highlights strong retention of the overall protein complexes and confirms notions made in prior literature in this regard.^{2,46–51} Further, the SRA supports prior reports^{46,50} that the charge states observed under native IM/MS measurements for the same protein complex exert only a negligible impact on the retention of native contacts. Finally, the dominant binding interfaces between polypeptide chains in the complexes studied here appear retained largely to the same extent as native contacts within the polypeptide chains. However, the SRA also indicates that significant loss of native contacts can occur for weakly binding interfaces (although this may depend on the specific protein complex) and for interfaces composed of terminal and untethered regions of polypeptide chains.

Compaction of Protein Systems Correlates Weakly with Retention of Native Contacts. A significant body of prior literature investigated structural reorganization of protein complexes that occur in the absence of solvent during the course of IM/MS measurements.^{2,46-51} A hallmark of native IM/MS of proteins and protein complexes is their "compaction" in the absence of solvent, i.e., the observation that the cross section measured by IM/MS can be up to \sim 20% smaller than the cross section calculated for the X-ray or NMR structures. This compaction is significant because it points to structural differences between the X-ray or NMR protein structure and its structure detected by IM/MS. Recently, Rolland et al. investigated compaction of several protein complexes by means of MD simulations and proposed that their compaction arises mainly from a smoothing of the protein surface due to self-solvation by amino acid side chains in the absence of solvent.⁵⁰ Nevertheless, at least for some charge states, compaction may be related to collapse of cavities and grooves of the protein. 50,52

The protein complexes studied here exhibit experimental cross sections that are up to $\sim\!26\%$ smaller than those calculated for the respective X-ray and/or NMR structures (see Figure 4 and Table S3, Supporting Information), which indicates compaction of these systems. The most significant compaction is observed for the dimers of CCL5 (26 and 22%, respectively, for charge states 7+ and 8+) and SOD1 (between 5 and 8% for charge states 11+ to 13+). The increased compaction for CCL5 dimers and SOD1 dimers can be

rationalized by the unstructured N-terminus of CCL5 in solution and the large regions that appear unstructured in solution for SOD1 dimers (see the Supporting Information, Figure S4). For the neutravidin and streptavidin tetramers, the experimental and computed cross sections are within the errors of the methods, and we hence conclude no compaction to occur for these systems.

Our data indicate that the degree of compaction is only weakly correlated with loss of native contacts (Figure 4b). As an example, the SOD1 dimer and the neutravidin tetramer retain a similar fraction of native contacts ($Q \sim 0.83$ and 0.87, respectively) while SOD1 compacts by ~8% neutravidin does not compact. Further, linear regression analysis of the data shown in Figure 4b suggests that protein complexes would still retain ~42% of their native contacts even if they were to compact by 100% (i.e., in the hypothetical limit of a vanishing cross section). Hence, our data underline that structural reorganization of protein backbone contacts is not the principal factor associated with compaction of protein systems in native IM/MS. Our data further establish that the degree of compaction within a series of charge states of the same protein system is unrelated to the extent to which backbone residueresidue interactions are retained: the fraction of native contacts decreases slightly with increasing charge state, whereas the compaction decreases (see Tables S2 and S3). These observations argue against the notion⁵² that protein ions with charge states that best match the cross section calculated for native X-ray/NMR structures may also be most native in structure.

Protein Structures Stabilize in the Absence of Solvent by Remodeling Their Surface to Modestly Increase Their Hydrophobic Content. To assess how strongly the structural reorganization of the protein complexes in IM/MS affects their surfaces, we calculated the solventaccessible surface areas 76,85 for the protein complexes as the means over the corresponding ensembles (Table 1). The tabulated values show that the surface area of each protein system decreases during IM/MS measurements by ~10 to ~25%. These overall changes in their surface areas appear uncorrelated with the degree to which native backbone residue-residue interactions are retained as well as the extent of the compaction. As an example, the SRA indicates that the surface area of neutravidin decreases by ~25% (Table 1) but the fraction of native contacts ($Q \sim 0.9$, see Figure 3 and Table S2, Supporting Information) indicates only negligible loss of native backbone contacts, and we found no indication for a compaction during IM/MS (Figure 4 and Tables S3 and S4 in the Supporting Information).

We next partitioned the surface areas into hydrophilic and hydrophobic contributions (Table 1). In line with prior literature, the data show that the hydrophobic surface area exceeds the hydrophilic area in solution (55 vs 45%, respectively). Our data further indicate that the hydrophobic surface area increases by only a modest 10% in the absence of solvent (65% hydrophobic vs 35% hydrophilic, respectively). What is further intriguing is that the ratios of hydrophilic vs hydrophobic surface areas in Table 1 cluster around 65–35%, irrespective of the protein system, assembly state, or charge state. Taken together, our analysis indicates that a reduction of the surface area by \sim 20% and a modest increase of the hydrophobic surface by \sim 10% appear to sufficiently stabilize a protein system in the absence of solvent so that its structure becomes metastable on the time scale of IM/MS measure-

Table 1. Mean Total Solvent-Accessible Surface Area (SASA) and the Hydrophilic and Hydrophobic Contribution to the SASA Calculated for the Solution-Phase Ensembles and the Corresponding Ensembles Predicted by the SRA for Each Charge State after Structure Relaxation in the Absence of Solvent

		solvent-accessible surface area (SASA)		
protein system	solution/charge state	total area (Ų)	hydrophilic (%)	hydrophobic (%)
CCL5	solution	9689	44	56
	7+	7418	33	67
	8+	7493	33	67
SOD1	solution	18,052	44	56
	11+	14,327	35	65
	12+	14,434	35	65
	13+	14,579	35	65
streptavidin	solution	26,461	43	57
	15+	22,699	35	65
	16+	23,086	35	65
	17+	23,498	35	65
	18+	23,888	35	65
neutravidin	solution	30,117	45	55
	17+	22,768	35	65
	18+	22,955	35	65
	19+	23,095	35	65

ments. This observation supports the proposition⁵⁰ that structure relaxation of protein systems in the absence of solvent may largely be associated with remodeling of the protein surface to increase the hydrophobic surface area. Further, the consistency between the different protein systems and charge states observed in Table 1 suggests that this remodeling process of the protein surface is not protein specific but may instead follow principles valid for various classes of protein systems.

Protein Surface Remodeling in the Absence of Solvent Is an Inherent Property of the Structural Relaxation Process Rather than Protein-Specific. Our discussion above supports prior work⁵⁰ that structural changes in the absence of solvent are mainly associated with remodeling of the protein surface. Further, the consistency of the ratio between hydrophilic and hydrophobic surface area for the different protein systems and charge states (Table 1) suggests that this protein surface remodeling may follow principles valid for various classes of protein systems. To assess if reorganization of the protein surface in the absence of solvent involves all amino acid residues equally or if surface reorganization is mainly an effect of specific proteins and/or certain residues, we calculated the change in the hydrophilic and hydrophobic surface area for each residue before and after gas-phase relaxation for each structure of the ensemble of each protein complex.

Figure 5 correlates the mean changes of the surface areas for each residue with their hydrophilic surface areas of the solution structure (for brevity and clarity, we limit our discussion to the lowest charge states of the systems studied here). The plots show that residues that expose large hydrophilic areas in the presence of the solvent undergo the strongest decrease of their hydrophilic and hydrophobic surface areas upon structural reorganization in the IM/MS experiment. Furthermore, Figure 5 shows that this correlation is to a first approximation linear and consistent between the different protein systems (see

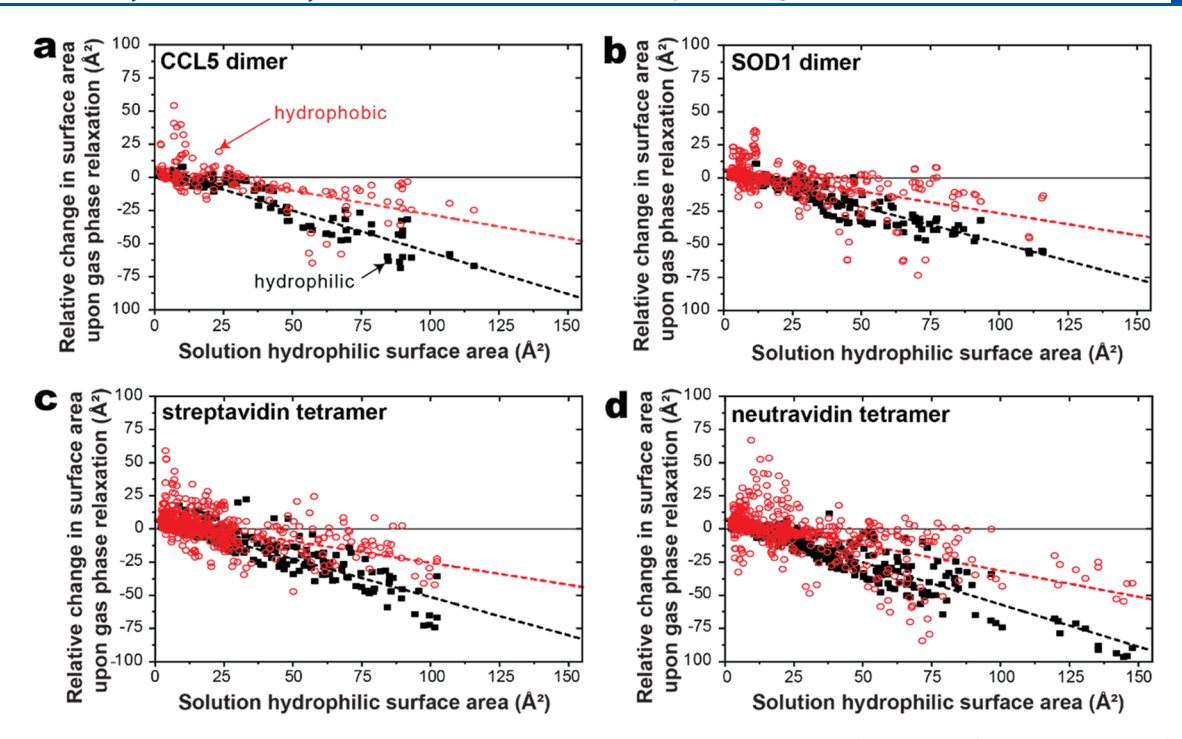


Figure 5. Correlation between the solution hydrophilic surface area and the change in hydrophilic (black square) and hydrophobic (red circle) surface area upon gas-phase relaxation per residue for (a) CCL5 dimers, (b) SOD1 dimers, (c) streptavidin tetramers, and (d) neutravidin tetramers. Solvent-exposed hydrophilic residues become buried upon gas-phase relaxation while the majority of residues do not experience significant changes in their surface area. Linear correlations between the solution hydrophilic surface area and the change in the hydrophilic (black dashed lines) and hydrophobic (red dashed lines) surface areas are comparable between the protein systems, which suggests that the processes underlying the surface remodeling in the absence of solvent may be of general nature and not protein-specific.

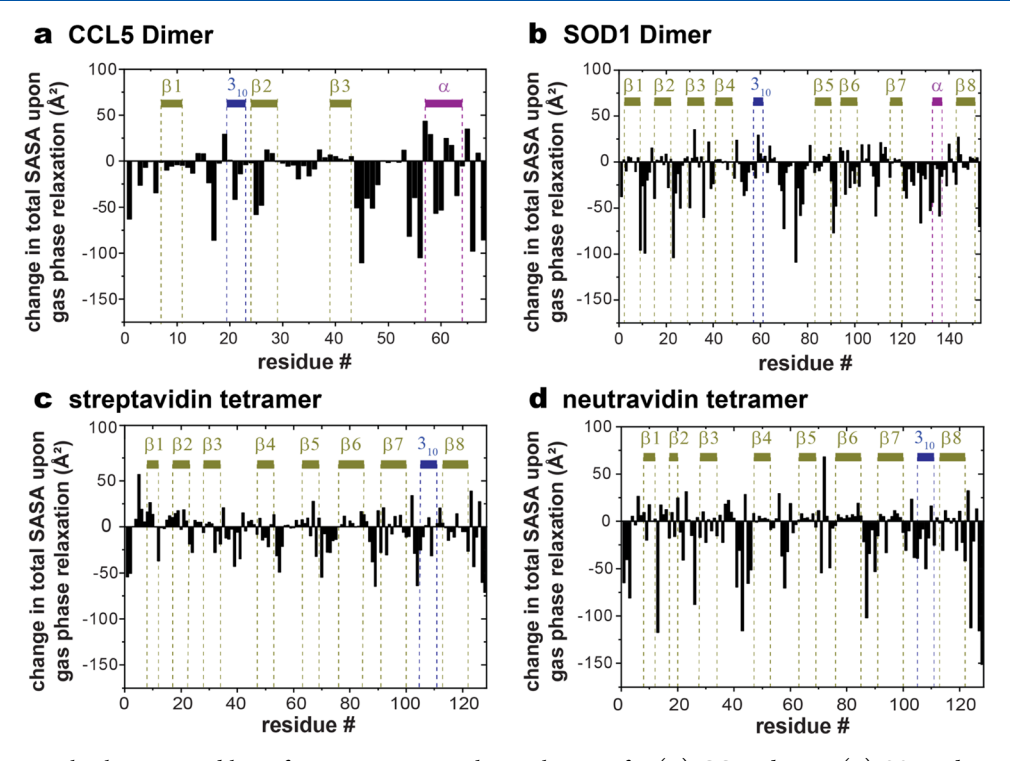


Figure 6. Change in total solvent-accessible surface area upon gas-phase relaxation for (A) CCL5 dimers, (B) SOD1 dimers, (C) streptavidin tetramers, and (D) neutravidin tetramers mapped onto the secondary structure elements. The plots indicate that residues with significant reduction in surface area are most often located outside of helical or β-strand secondary structure elements.

Table S5, Supporting Information). We draw two conclusions from these observations: First, these observations support our discussion above and prior work⁵⁰ that reasoned that structural

reorganization of the protein surface is associated mainly with self-solvation of amino acid residues exposing large hydrophilic surface areas to the solvent. Second, linear regression analysis shows that the correlations between the change in hydrophobic and hydrophilic contributions to the solvent-accessible surface area and the solution hydrophilic surface area are similar for all protein complexes (see Table S5, Supporting Information). Furthermore, the low abundance of acidic and basic residues exposed on the protein surfaces argues against the notion that remodeling of the protein's surface is significantly informed by formation of salt bridges of the protein surfaces (see the Supporting Information, Figures S5 and S6). Taken together, these observations underline that remodeling of the protein surface upon removal of solvent is likely an inherent property of the structural relaxation process rather than protein-specific.

To identify if the decrease in surface area is associated with specific structural regions of the protein, we mapped the change in surface area for each residue to the position of the residue and its secondary structure element (Figure 6). Figure 6 indicates that residues with significant reduction in surface area are most often located outside of helical or β -strand secondary structure elements. We next classified the residues per their secondary structure region (helical, β -strand, other) and found that residues located outside of helical or β -strand secondary structure elements contribute to the reduction of the surface area significantly more strongly than residues located within secondary structure elements (Figure 7). (Note

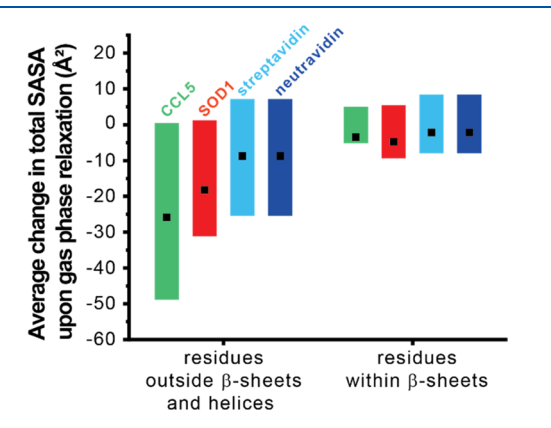


Figure 7. Mean per residue change in solvent-accessible surface area upon structural relaxation in the absence of solvent outside classified by secondary structure type for CCL5 dimers (green bars), SOD1 dimers (red bars), streptavidin tetramers (light blue bars), and neutravidin tetramers (dark blue bars). Black squares indicate the average change in surface area, while the length of each bar indicated the standard deviation of the distribution. Residues that undergo a significant reduction of their surface areas are most often located outside of helical or β -strand secondary structure, whereas β -strand elements are found to only marginally contribute to the remodeling of the surface area.

that the limited number of helical components in the protein complexes studied here prevents a statistically meaningful analysis of these residues.) Taken together, our analysis suggests that remodeling of the protein surface in the absence of solvent is mainly due to structural reorganization of (hydrophilic) residues located outside of β -strand secondary structure elements. We note that this observation is consistent with the notion that β -sheet propensity is mainly driven by entropic factors in solution, ⁸⁷ because this means that β -sheet propensity should, to a first approximation, not be affected by removal of solvent.

Protein Surface Remodeling Is Uncorrelated to Changes in Protein Volume and Void Volume. Our

discussion above highlights that protein structures stabilize in the absence of solvent via increasing the hydrophobic content of their surface area by ~10% (Table 1). In line with prior work, ⁵⁰ our data here suggest that this restructuring of the protein surface is accomplished largely by the folding of solvent-exposed, hydrophilic side chains onto the protein scaffold not part of helical and β -strand secondary structure elements (Figures 5 and 6).

To assess to what extent the internal structural organization of the protein (i.e., packing of atoms and presence of cavities or grooves within the protein scaffold) is affected by the restructuring of the protein surface, we calculated the changes to the mean total volumes, packing densities, and void volumes of the protein systems. The values are listed in Table S6 (Supporting Information) and indicate no significant differences between the volumes of the protein solution ensembles and those of the SRA-predicted ensembles for the various charge states in the absence of solvent. This finding runs counter to the idea of a simple geometrical contraction or tightening of the protein scaffold upon removal of solvent. The packing density, defined as the ratio of the van der Waals volume and total (molecular) volume, is a rough measure for the flexibility of the polypeptide chain where a denser packing corresponds to lower flexibility. The packing density calculated for the solvated protein systems varies between 0.72 and 0.75, which is in the range expected for protein systems. 85 The SRA indicates that the packing density changes negligibly in the absence of solvent (see Table S6, Supporting Information). Hence, our analysis suggests that structural changes occurring during IM/MS measurements do not significantly alter the internal flexibility of the polypeptide chain. This finding further argues against protein compaction in the absence of solvent arising from a geometrical tightening of the protein solution structure. We calculated the mean void volumes for the solution ensemble and the SRA-predicted ensembles for the various charge states to identify the extent to which cavities in the protein scaffold change during an IM/MS measurement. The data listed in Table S6 (Supporting Information) indicate only minor differences between the void volumes of the solution and IM/MS ensembles, underlining that cavities or grooves appear retained. Because the void volume has been used as an indicator for the pressure and thermal stability of proteins, this observation further supports the notion that the internal structures of the protein systems studied here appear marginally affected by the remodeling of the protein surface in the absence of solvent on the time scale of IM/MS measurements.

CONCLUSIONS

We used the structure relaxation approximation (SRA) to structurally interpret ion mobility spectra for several protein complexes in the range from $\sim\!\!16$ to $\sim\!\!60$ kDa and charge states from +7 to +19. We found that the IM/MS spectra predicted by the SRA method agreed with the experimental spectra within the errors of the methods. The SRA indicates the following:

- (1) Native backbone residue—residue interactions appear largely retained in the absence of solvent for the investigated protein complexes and charge states.
- (2) Strongly binding interfaces between polypeptide chains, such as those within a dimer subunit of the streptavidin

tetramer complex, appear largely retained in IM/MS measurements.

- (3) Retention of interfaces between different subunits of protein complexes appears to be system-dependent and strongly retained in some systems (i.e., binding between two neutravidin dimer subunits) but less so in others (i.e., binding between two streptavidin dimer subunits).
- (4) Structural reorganization of the protein systems in IM/ MS measurements appears largely driven by remodeling of the protein surface and associated with only a modest 10% increase in the hydrophobic surface area with respect to their solution structures.
- (5) Surface-bound, non-native salt bridges formed in the absence of solvent do not appear to play a major role in the remodeling of the protein surfaces.
- (6) Remodeling of the protein surface appears to be an inherent property of the structural relaxation and stabilization process in the absence of solvent rather than protein-specific.
- (7) The hallmark compaction often observed for protein systems in native IM/MS measurements appears to be a poor indicator of the extent to which native residue residue interactions are retained in the absence of solvent.
- (8) The packing densities and void volumes of the protein complexes studied here appear unaltered by the structural reorganization of the protein systems in the absence of solvent, regardless of charge state. This suggests that the internal structure of protein systems may be largely retained on the time scale of IM/MS measurements.

We conclude that the SRA indicates that structural changes occurring in the absence of solvent on the time scale of IM/MS measurements appear largely associated with remodeling of the protein surface to increase the hydrophobic surface area by ~10%. Our analysis indicates that superficial changes mainly of those residues not part of β -strand secondary structure elements appear to be sufficient to achieve this restructuring of the protein surface and lead to metastability of the protein structures on the time scale of IM/MS experiments.

ASSOCIATED CONTENT

Supporting Information

The Supporting Information is available free of charge at https://pubs.acs.org/doi/10.1021/acs.jpcb.3c01024.

Expanded experimental and computational details; two schematics of the tandem-trapped ion mobility spectrometer/mass spectrometer; four figures related to analysis of the SRA calculations; and five tables with cross section for main features measured experimentally and computationally, fraction of native contacts, degree of compaction, and analysis of the volumes of predicted structures (PDF)

AUTHOR INFORMATION

Corresponding Author

Christian Bleiholder — Department of Chemistry and Biochemistry, Florida State University, Tallahassee, Florida 32306, United States; Institute of Molecular Biophysics, Florida State University, Tallahassee, Florida 32306, United States; o orcid.org/0000-0002-4211-1388; Phone: +1-850-645-4816; Email: cbleiholder@fsu.edu

Authors

- Tyler C. Cropley Department of Chemistry and Biochemistry, Florida State University, Tallahassee, Florida 32306, United States; oorcid.org/0000-0003-2804-2555
- Fanny C. Liu Department of Chemistry and Biochemistry, Florida State University, Tallahassee, Florida 32306, United States; © orcid.org/0000-0003-1403-7114
- Thais Pedrete Department of Chemistry and Biochemistry, Florida State University, Tallahassee, Florida 32306, United States
- Md Amin Hossain Department of Chemistry and Chemical Biology, Northeastern University, Boston, Massachusetts 02115, United States; Barnett Institute of Chemical and Biological Analysis, Boston, Massachusetts 02115, United States
- Jeffrey N. Agar Department of Chemistry and Chemical Biology, Northeastern University, Boston, Massachusetts 02115, United States; Barnett Institute of Chemical and Biological Analysis, Boston, Massachusetts 02115, United States; Department of Pharmaceutical Sciences, Northeastern University, Boston, Massachusetts 02115, United States

Complete contact information is available at: https://pubs.acs.org/10.1021/acs.jpcb.3c01024

Author Contributions

*T.C.C. and F.C.L. contributed equally to this work. The manuscript was written through contributions of all authors. All authors have given approval to the final version of the manuscript.

Notes

The authors declare no competing financial interest.

ACKNOWLEDGMENTS

This work was supported by the National Science Foundation under grant CHE-1654608 (C.B.).

ABBREVIATIONS

IM/MS, ion mobility/mass spectrometry; SRA, structure relaxation approximation; tTIMS/MS, tandem-trapped ion mobility spectrometer/mass spectrometer; ESI, electrospray ionization; TIMS, trapped ion mobility spectrometry; MD, molecular dynamics; PSA, projection superposition approximation; Q, fraction of native contacts; CCLS, C—C motif ligand 5; SOD1, Superoxide dismutase type 1

REFERENCES

- (1) Marsh, J. A.; Teichmann, S. A. Structure, Dynamics, Assembly, and Evolution of Protein Complexes. *Annu. Rev. Biochem.* **2015**, *84*, 551–575.
- (2) Zhou, M.; Politis, A.; Davies, R. B.; Liko, I.; Wu, K.-J.; Stewart, A. G.; Stock, D.; Robinson, C. V. Ion Mobility—Mass Spectrometry of a Rotary ATPase Reveals ATP-Induced Reduction in Conformational Flexibility. *Nat. Chem.* **2014**, *6*, 208–215.
- (3) Acuner Ozbabacan, S. E.; Engin, H. B.; Gursoy, A.; Keskin, O. Transient Protein-Protein Interactions. *Protein Eng. Des. Sel.* **2011**, *24*, 635–648.
- (4) Ramakrishnan, V. Ribosome Structure and the Mechanism of Translation. *Cell* **2002**, *108*, 557–572.
- (5) Nissim, S.; Leshchiner, I.; Mancias, J. D.; Greenblatt, M. B.; Maertens, O.; Cassa, C. A.; Rosenfeld, J. A.; Cox, A. G.; Hedgepeth, J.; Wucherpfennig, J. I.; et al. Mutations in RABL3 Alter KRAS

- Prenylation and Are Associated with Hereditary Pancreatic Cancer. *Nat. Genet.* **2019**, *51*, 1308–1314.
- (6) Zhong, X.; Su, L.; Yang, Y.; Nair-Gill, E.; Tang, M.; Anderton, P.; Li, X.; Wang, J.; Zhan, X.; Tomchick, D. R.; Brautigam, C. A.; et al. Genetic and Structural Studies of RABL3 Reveal an Essential Role in Lymphoid Development and Function. *Proc. Natl. Acad. Sci. U.S.A.* 2020, 117, 8563–8572.
- (7) Razavi, H.; Palaninathan, S. K.; Powers, E. T.; Wiseman, R. L.; Purkey, H. E.; Mohamedmohaideen, N. N.; Deechongkit, S.; Chiang, K. P.; Dendle, M. T. A.; Sacchettini, J. C.; Kelly, J. W. Benzoxazoles as Transthyretin Amyloid Fibril Inhibitors: Synthesis, Evaluation, and Mechanism of Action. *Angew. Chem., Int. Ed.* 2003, 42, 2758–2761.
- (8) Larion, M.; Hansen, A. L.; Zhang, F.; Bruschweiler-Li, L.; Tugarinov, V.; Miller, B. G.; Brüschweiler, R. Kinetic Cooperativity in Human Pancreatic Glucokinase Originates from Millisecond Dynamics of the Small Domain. *Angew. Chem.* **2015**, *127*, 8247–8250.
- (9) Cole, R.; Loria, J. P. Evidence for Flexibility in the Function of Ribonuclease A. *Biochemistry* **2002**, *41*, 6072–6081.
- (10) Watt, E. D.; Shimada, H.; Kovrigin, E. L.; Loria, J. P. The Mechanism of Rate-Limiting Motions in Enzyme Function. *Proc. Natl. Acad. Sci. U.S.A.* **2007**, *104*, 11981–11986.
- (11) Lisi, G. P.; Loria, J. P. Solution NMR Spectroscopy for the Study of Enzyme Allostery. *Chem. Rev.* **2016**, *116*, 6323–6369.
- (12) Alderson, T. R.; Kay, L. E. NMR Spectroscopy Captures the Essential Role of Dynamics in Regulating Biomolecular Function. *Cell* **2021**, *184*, 577–595.
- (13) McAlary, L.; Aquilina, J. A.; Yerbury, J. J. Susceptibility of Mutant SOD1 to Form a Destabilized Monomer Predicts Cellular Aggregation and Toxicity but Not In Vitro Aggregation Propensity. *Front. Neurosci.* **2016**, *10*, No. 499.
- (14) Klein, W. L.; Stine, W. B.; Teplow, D. B. Small Assemblies of Unmodified Amyloid β -Protein Are the Proximate Neurotoxin in Alzheimer's Disease. *Neurobiol. Aging* **2004**, 25, 569–580.
- (15) Koenen, R. R.; von Hundelshausen, P.; Nesmelova, I. V.; Zernecke, A.; Liehn, E. A.; Sarabi, A.; Kramp, B. K.; Piccinini, A. M.; Paludan, S. R.; Kowalska, M. A.; et al. Disrupting Functional Interactions between Platelet Chemokines Inhibits Atherosclerosis in Hyperlipidemic Mice. *Nat. Med.* **2009**, *15*, 97–103.
- (16) Allen, S. J.; Crown, S. E.; Handel, T. M. Chemokine:Receptor Structure, Interactions, and Antagonism. *Annu. Rev. Immunol.* **2007**, 25, 787–820.
- (17) Thelen, M.; Stein, J. V. How Chemokines Invite Leukocytes to Dance. *Nat. Immunol.* **2008**, *9*, 953–959.
- (18) Bernstein, S. L.; Dupuis, N. F.; Lazo, N. D.; Wyttenbach, T.; Condron, M. M.; Bitan, G.; Teplow, D. B.; Shea, J.-E.; Ruotolo, B. T.; Robinson, C. V.; Bowers, M. T. Amyloid- β Protein Oligomerization and the Importance of Tetramers and Dodecamers in the Aetiology of Alzheimer's Disease. *Nat. Chem.* **2009**, *1*, 326–331.
- (19) Bleiholder, C.; Dupuis, N. F.; Wyttenbach, T.; Bowers, M. T. Ion Mobility–Mass Spectrometry Reveals a Conformational Conversion from Random Assembly to β -Sheet in Amyloid Fibril Formation. *Nat. Chem.* **2011**, *3*, 172–177.
- (20) Young, L. M.; Cao, P.; Raleigh, D. P.; Ashcroft, A. E.; Radford, S. E. Ion Mobility Spectrometry–Mass Spectrometry Defines the Oligomeric Intermediates in Amylin Amyloid Formation and the Mode of Action of Inhibitors. *J. Am. Chem. Soc.* **2014**, *136*, 660–670.
- (21) Bleiholder, C.; Bowers, M. T. The Solution Assembly of Biological Molecules Using Ion Mobility Methods: From Amino Acids to Amyloid β -Protein. *Annu. Rev. Anal. Chem.* **2017**, *10*, 365–386
- (22) Havugimana, P. C.; Hart, G. T.; Nepusz, T.; Yang, H.; Turinsky, A. L.; Li, Z.; Wang, P. I.; Boutz, D. R.; Fong, V.; Phanse, S.; Babu, M.; et al. A Census of Human Soluble Protein Complexes. *Cell* **2012**, *150*, 1068–1081.
- (23) Vidal, M.; Cusick, M. E.; Barabási, A.-L. Interactome Networks and Human Disease. *Cell* **2011**, *144*, 986–998.
- (24) Richards, A. L.; Eckhardt, M.; Krogan, N. J. Mass Spectrometry-based Protein Protein Interaction Networks for the Study of Human Diseases. *Mol. Syst. Biol.* **2021**, *17*, No. e8792.

- (25) Pankow, S.; Bamberger, C.; Calzolari, D.; Martínez-Bartolomé, S.; Lavallée-Adam, M.; Balch, W. E.; Yates, J. R. ΔF508 CFTR Interactome Remodelling Promotes Rescue of Cystic Fibrosis. *Nature* **2015**, 528, 510–516.
- (26) Gavin, A.-C.; Bösche, M.; Krause, R.; Grandi, P.; Marzioch, M.; Bauer, A.; Schultz, J.; Rick, J. M.; Michon, A.-M.; Cruciat, C.-M.; et al. Functional Organization of the Yeast Proteome by Systematic Analysis of Protein Complexes. *Nature* **2002**, *415*, 141–147.
- (27) Aebersold, R.; Mann, M. Mass-Spectrometric Exploration of Proteome Structure and Function. *Nature* **2016**, *537*, 347–355.
- (28) Aebersold, R.; Agar, J. N.; Amster, I. J.; Baker, M. S.; Bertozzi, C. R.; Boja, E. S.; Costello, C. E.; Cravatt, B. F.; Fenselau, C.; Garcia, B. A.; et al. How Many Human Proteoforms Are There? *Nat. Chem. Biol.* 2018, 14, 206–214.
- (29) Limbach, P. A.; Grosshans, P. B.; Marshall, A. G. Experimental Determination of the Number of Trapped Ions, Detection Limit, and Dynamic Range in Fourier Transform Ion Cyclotron Resonance Mass Spectrometry. *Anal. Chem.* **1993**, *65*, 135–140.
- (30) Meier, F.; Brunner, A.-D.; Frank, M.; Ha, A.; Bludau, I.; Voytik, E.; Kaspar-Schoenefeld, S.; Lubeck, M.; Raether, O.; Bache, N.; et al. DiaPASEF: Parallel Accumulation—Serial Fragmentation Combined with Data-Independent Acquisition. *Nat. Methods* **2020**, *17*, 1229—1236.
- (31) Baker, E. S.; Burnum-Johnson, K. E.; Ibrahim, Y. M.; Orton, D. J.; Monroe, M. E.; Kelly, R. T.; Moore, R. J.; Zhang, X.; Théberge, R.; Costello, C. E.; Smith, R. D. Enhancing Bottom-up and Top-down Proteomic Measurements with Ion Mobility Separations. *Proteomics* 2015, 15, 2766–2776.
- (32) Deng, L.; Webb, I. K.; Garimella, S. V. B.; Hamid, A. M.; Zheng, X.; Norheim, R. V.; Prost, S. A.; Anderson, G. A.; Sandoval, J. A.; Baker, E. S.; et al. Serpentine Ultralong Path with Extended Routing (SUPER) High Resolution Traveling Wave Ion Mobility-MS Using Structures for Lossless Ion Manipulations. *Anal. Chem.* **2017**, *89*, 4628–4634.
- (33) Benesch, J. L. P.; Ruotolo, B. T.; Simmons, D. A.; Robinson, C. V. Protein Complexes in the Gas Phase: Technology for Structural Genomics and Proteomics. *Chem. Rev.* **2007**, *107*, 3544–3567.
- (34) Kondrat, F. D. L.; Struwe, W. B.; Benesch, J. L. P. Native Mass Spectrometry: Towards High-Throughput Structural Proteomics. In *Structural Proteomics*; Owens, R. J., Ed.; Methods in Molecular Biology; Springer: New York, NY, 2015; Vol. *1261*, pp 349–371.
- (35) Breuker, K.; McLafferty, F. W. Stepwise Evolution of Protein Native Structure with Electrospray into the Gas Phase, 10^{-12} to 10^{2} s. *Proc. Natl. Acad. Sci. U.S.A.* **2008**, *105*, 18145–18152.
- (36) Wolynes, P. G. Biomolecular Folding in Vacuo!!!(?). *Proc. Natl. Acad. Sci. U.S.A.* **1995**, 92, 2426–2427.
- (37) Bleiholder, C.; Liu, F. C. Structure Relaxation Approximation (SRA) for Elucidation of Protein Structures from Ion Mobility Measurements. *J. Phys. Chem. B* **2019**, 123, 2756–2769.
- (38) Wyttenbach, T.; Bowers, M. T. Structural Stability from Solution to the Gas Phase: Native Solution Structure of Ubiquitin Survives Analysis in a Solvent-Free Ion Mobility—Mass Spectrometry Environment. *J. Phys. Chem. B* **2011**, *115*, 12266—12275.
- (39) Chai, M.; Bleiholder, C. Structure-Elucidation of Human CCL5 by Integrating Trapped Ion Mobility Spectrometry-Mass Spectrometry (TIMS-MS) with Structure Relaxation Approximation (SRA) Analysis. *Int. J. Mass Spectrom.* **2021**, 469, No. 116682.
- (40) Myung, S.; Badman, E. R.; Lee, Y. J.; Clemmer, D. E. Structural Transitions of Electrosprayed Ubiquitin Ions Stored in an Ion Trap over ~10 Ms to 30 s. *J. Phys. Chem. A* **2002**, *106*, 9976–9982.
- (41) Allen, S. J.; Eaton, R. M.; Bush, M. F. Structural Dynamics of Native-Like Ions in the Gas Phase: Results from Tandem Ion Mobility of Cytochrome *c. Anal. Chem.* **2017**, *89*, 7527–7534.
- (42) Laszlo, K. J.; Munger, E. B.; Bush, M. F. Folding of Protein Ions in the Gas Phase after Cation-to-Anion Proton-Transfer Reactions. *J. Am. Chem. Soc.* **2016**, *138*, 9581–9588.
- (43) Jhingree, J. R.; Beveridge, R.; Dickinson, E. R.; Williams, J. P.; Brown, J. M.; Bellina, B.; Barran, P. E. Electron Transfer with No Dissociation Ion Mobility–Mass Spectrometry (ETnoD IM-MS).

- The Effect of Charge Reduction on Protein Conformation. *Int. J. Mass Spectrom.* **2017**, *413*, 43–51.
- (44) Koeniger, S. L.; Merenbloom, S. I.; Sevugarajan, S.; Clemmer, D. E. Transfer of Structural Elements from Compact to Extended States in Unsolvated Ubiquitin. *J. Am. Chem. Soc.* **2006**, *128*, 11713–11719.
- (45) Jurneczko, E.; Barran, P. E. How Useful Is Ion Mobility Mass Spectrometry for Structural Biology? The Relationship between Protein Crystal Structures and Their Collision Cross Sections in the Gas Phase. *Analyst* **2011**, *136*, 20–28.
- (46) Bush, M. F.; Hall, Z.; Giles, K.; Hoyes, J.; Robinson, C. V.; Ruotolo, B. T. Collision Cross Sections of Proteins and Their Complexes: A Calibration Framework and Database for Gas-Phase Structural Biology. *Anal. Chem.* **2010**, *82*, 9557–9565.
- (47) Quintyn, R. S.; Yan, J.; Wysocki, V. H. Surface-Induced Dissociation of Homotetramers with D2 Symmetry Yields Their Assembly Pathways and Characterizes the Effect of Ligand Binding. *Chem. Biol.* **2015**, *22*, 583–592.
- (48) Stiving, A. Q.; VanAernum, Z. L.; Busch, F.; Harvey, S. R.; Sarni, S. H.; Wysocki, V. H. Surface-Induced Dissociation: An Effective Method for Characterization of Protein Quaternary Structure. *Anal. Chem.* **2019**, *91*, 190–209.
- (49) Loo, J. A. Studying Noncovalent Protein Complexes by Electrospray Ionization Mass Spectrometry. *Mass Spectrom. Rev.* **1997**, *16*, 1–23.
- (50) Rolland, A. D.; Biberic, L. S.; Prell, J. S. Investigation of Charge-State-Dependent Compaction of Protein Ions with Native Ion Mobility—Mass Spectrometry and Theory. *J. Am. Soc. Mass Spectrom.* **2022**, *33*, 369–381.
- (51) Ruotolo, B. T.; Giles, K.; Campuzano, I.; Sandercock, A. M.; Bateman, R. H.; Robinson, C. V. Evidence for Macromolecular Protein Rings in the Absence of Bulk Water. *Science* **2005**, *310*, 1658–1661.
- (52) Hall, Z.; Politis, A.; Bush, M. F.; Smith, L. J.; Robinson, C. V. Charge-State Dependent Compaction and Dissociation of Protein Complexes: Insights from Ion Mobility and Molecular Dynamics. *J. Am. Chem. Soc.* **2012**, *134*, 3429–3438.
- (53) France, A. P.; Migas, L. G.; Sinclair, E.; Bellina, B.; Barran, P. E. Using Collision Cross Section Distributions to Assess the Distribution of Collision Cross Section Values. *Anal. Chem.* **2020**, *92*, 4340–4348.
- (54) Shvartsburg, A. A.; Jarrold, M. F. An Exact Hard-Spheres Scattering Model for the Mobilities of Polyatomic Ions. *Chem. Phys. Lett.* **1996**, *261*, 86–91.
- (55) Wyttenbach, T.; von Helden, G.; Batka, J. J.; Carlat, D.; Bowers, M. T. Effect of the Long-Range Potential on Ion Mobility Measurements. J. Am. Soc. Mass Spectrom. 1997, 8, 275–282.
- (56) Bleiholder, C.; Wyttenbach, T.; Bowers, M. T. A Novel Projection Approximation Algorithm for the Fast and Accurate Computation of Molecular Collision Cross Sections (I). Method. *Int. J. Mass Spectrom.* **2011**, 308, 1–10.
- (57) Bonner, J.; Lyon, Y. A.; Nellessen, C.; Julian, R. R. Photoelectron Transfer Dissociation Reveals Surprising Favorability of Zwitterionic States in Large Gaseous Peptides and Proteins. *J. Am. Chem. Soc.* **2017**, *139*, 10286–10293.
- (58) Loo, R. R. O.; Loo, J. A. Salt Bridge Rearrangement (SaBRe) Explains the Dissociation Behavior of Noncovalent Complexes. *J. Am. Soc. Mass Spectrom.* **2016**, *27*, 975–990.
- (59) Gao, B.; Wyttenbach, T.; Bowers, M. T. Hydration of Protonated Aromatic Amino Acids: Phenylalanine, Tryptophan, and Tyrosine. J. Am. Chem. Soc. 2009, 131, 4695–4701.
- (60) Grandori, R. Origin of the Conformation Dependence of Protein Charge-State Distributions in Electrospray Ionization Mass Spectrometry. J. Mass Spectrom. 2003, 38, 11–15.
- (61) Kjeldsen, F.; Silivra, O. A.; Zubarev, R. A. Zwitterionic States in Gas-Phase Polypeptide Ions Revealed by 157-nm Ultra-Violet Photodissociation. *Chem. Eur. J.* **2006**, *12*, 7920–7928.
- (62) Westphall, M. S.; Lee, K. W.; Salome, A. Z.; Lodge, J. M.; Grant, T.; Coon, J. J. Three-Dimensional Structure Determination of

- Protein Complexes Using Matrix-Landing Mass Spectrometry. *Nat. Commun.* **2022**, *13*, No. 2276.
- (63) Rinke, G.; Rauschenbach, S.; Schrettl, S.; Hoheisel, T. N.; Blohm, J.; Gutzler, R.; Rosei, F.; Frauenrath, H.; Kern, K. Soft-Landing Electrospray Ion Beam Deposition of Sensitive Oligoynes on Surfaces in Vacuum. *Int. J. Mass Spectrom.* **2015**, 377, 228–234.
- (64) You, Z.; Cao, X.; Taylor, A. B.; Hart, P. J.; Levine, R. L. Characterization of a Covalent Polysulfane Bridge in Copper–Zinc Superoxide Dismutase. *Biochemistry* **2010**, *49*, 1191–1198.
- (65) Taylor, D. M.; Gibbs, B. F.; Kabashi, E.; Minotti, S.; Durham, H. D.; Agar, J. N. Tryptophan 32 Potentiates Aggregation and Cytotoxicity of a Copper/Zinc Superoxide Dismutase Mutant Associated with Familial Amyotrophic Lateral Sclerosis. *J. Biol. Chem.* **2007**, 282, 16329–16335.
- (66) Liu, F. C.; Ridgeway, M. E.; Park, M. A.; Bleiholder, C. Tandem Trapped Ion Mobility Spectrometry. *Analyst* **2018**, *143*, 2249–2258.
- (67) Liu, F. C.; Cropley, T. C.; Ridgeway, M. E.; Park, M. A.; Bleiholder, C. Structural Analysis of the Glycoprotein Complex Avidin by Tandem-Trapped Ion Mobility Spectrometry—Mass Spectrometry (Tandem-TIMS/MS). *Anal. Chem.* **2020**, *92*, 4459–4467.
- (68) Hernandez, D. R.; DeBord, J. D.; Ridgeway, M. E.; Kaplan, D. A.; Park, M. A.; Fernandez-Lima, F. Ion Dynamics in a Trapped Ion Mobility Spectrometer. *Analyst* **2014**, *139*, 1913–1921.
- (69) Chai, M.; Young, M. N.; Liu, F. C.; Bleiholder, C. A Transferable, Sample-Independent Calibration Procedure for Trapped Ion Mobility Spectrometry (TIMS). *Anal. Chem.* **2018**, *90*, 9040–9047.
- (70) Stow, S. M.; Causon, T. J.; Zheng, X.; Kurulugama, R. T.; Mairinger, T.; May, J. C.; Rennie, E. E.; Baker, E. S.; Smith, R. D.; McLean, J. A.; et al. An Interlaboratory Evaluation of Drift Tube Ion Mobility—Mass Spectrometry Collision Cross Section Measurements. *Anal. Chem.* **2017**, *89*, 9048—9055.
- (71) Duan, Y.; Wu, C.; Chowdhury, S.; Lee, M. C.; Xiong, G.; Zhang, W.; Yang, R.; Cieplak, P.; Luo, R.; Lee, T.; et al. A Point-Charge Force Field for Molecular Mechanics Simulations of Proteins Based on Condensed-Phase Quantum Mechanical Calculations. *J. Comput. Chem.* **2003**, 24, 1999–2012.
- (72) Jorgensen, W. L.; Chandrasekhar, J.; Madura, J. D.; Impey, R. W.; Klein, M. L. Comparison of Simple Potential Functions for Simulating Liquid Water. *J. Chem. Phys.* **1983**, *79*, 926–935.
- (73) Jorgensen, W. L.; Tirado-Rives, J. The OPLS Potential Functions for Proteins. Energy Minimizations for Crystals of Cyclic Peptides and Crambin. J. Am. Chem. Soc. 1988, 110, 1657–1666.
- (74) Kaminski, G. A.; Friesner, R. A.; Tirado-Rives, J.; Jorgensen, W. L. Evaluation and Reparametrization of the OPLS-AA Force Field for Proteins via Comparison with Accurate Quantum Chemical Calculations on Peptides. J. Phys. Chem. B 2001, 105, 6474–6487.
- (75) Segev, E.; Wyttenbach, T.; Bowers, M. T.; Gerber, R. B. Conformational Evolution of Ubiquitin Ions in Electrospray Mass Spectrometry: Molecular Dynamics Simulations at Gradually Increasing Temperatures. *Phys. Chem. Chem. Phys.* **2008**, *10*, 3077.
- (76) Fraternali, F. Parameter Optimized Surfaces (POPS): Analysis of Key Interactions and Conformational Changes in the Ribosome. *Nucleic Acids Res.* **2002**, *30*, 2950–2960.
- (77) Stewart, J. J. P. MOPAC2016; Stewart Computational Chemistry; Colorado Springs: CO, USA, 2016.
- (78) Chen, C. R.; Makhatadze, G. I. ProteinVolume: Calculating Molecular van Der Waals and Void Volumes in Proteins. *BMC Bioinf.* **2015**, *16*, 101.
- (79) Anderson, S. E.; Bleiholder, C.; Brocker, E. R.; Stang, P. J.; Bowers, M. T. A Novel Projection Approximation Algorithm for the Fast and Accurate Computation of Molecular Collision Cross Sections (III): Application to Supramolecular Coordination-Driven Assemblies with Complex Shapes. *Int. J. Mass Spectrom.* **2012**, 330–332, 78–84.
- (80) Bleiholder, C.; Contreras, S.; Do, T. D.; Bowers, M. T. A Novel Projection Approximation Algorithm for the Fast and Accurate Computation of Molecular Collision Cross Sections (II). Model

- Parameterization and Definition of Empirical Shape Factors for Proteins. *Int. J. Mass Spectrom.* **2013**, 345–347, 89–96.
- (81) Bleiholder, C.; Contreras, S.; Bowers, M. T. A Novel Projection Approximation Algorithm for the Fast and Accurate Computation of Molecular Collision Cross Sections (IV). Application to Polypeptides. *Int. J. Mass Spectrom.* **2013**, 354–355, 275–280.
- (82) Bleiholder, C.; Johnson, N. R.; Contreras, S.; Wyttenbach, T.; Bowers, M. T. Molecular Structures and Ion Mobility Cross Sections: Analysis of the Effects of He and N $_2$ Buffer Gas. *Anal. Chem.* **2015**, 87, 7196–7203.
- (83) Hall, Z.; Robinson, C. V. Do Charge State Signatures Guarantee Protein Conformations? *J. Am. Soc. Mass Spectrom.* **2012**, 23, 1161–1168.
- (84) Best, R. B.; Hummer, G.; Eaton, W. A. Native Contacts Determine Protein Folding Mechanisms in Atomistic Simulations. *Proc. Natl. Acad. Sci. U.S.A.* **2013**, *110*, 17874–17879.
- (85) Richards, F. M. The Interpretation of Protein Structures: Total Volume, Group Volume Distributions and Packing Density. *J. Mol. Biol.* **1974**, 82, 1–14.
- (86) Eisenhaber, F.; Argos, P. Hydrophobic Regions on Protein Surfaces: Definition Based on Hydration Shell Structure and a Quick Method for Their Computation. *Protein Eng., Des. Sel.* **1996**, *9*, 1121–1133.
- (87) Pal, D.; Chakrabarti, P. β -Sheet Propensity and Its Correlation Withparameters Based on Conformation. *Acta Crystallogr., Sect. D: Biol. Crystallogr.* **2000**, *56*, 589–594.